

Performance enhancement of sub-nanosecond diode-pumped passively Q-switched Yb:YAG microchip laser with diamond surface cooling

W. Z. Zhuang, Yi-Fan Chen, K. W. Su, K. F. Huang, and Y. F. Chen*

Department of Electrophysics, National Chiao Tung University, Hsinchu, Taiwan

*yfchen@cc.nctu.edu.tw

Abstract: We experimentally confirm that diamond surface cooling can significantly enhance the output performance of a sub-nanosecond diode-end-pumped passively Q-switched Yb:YAG laser. It is found that the pulse energy obtained with diamond cooling is approximately 1.5 times greater than that obtained without diamond cooling, where a Cr⁴⁺:YAG absorber with the initial transmission of 84% is employed. Furthermore, the standard deviation of the pulse amplitude peak-to-peak fluctuation is found to be approximately 3 times lower than that measured without diamond cooling. Under a pump power of 3.9 W, the passively Q-switched Yb:YAG laser can generate a pulse train of 3.3 kHz repetition rate with a pulse energy of 287 μ J and with a pulse width of 650 ps.

©2012 Optical Society of America

OCIS codes: (140.3480) Lasers, diode-pumped; (140.3320) Laser cooling; (140.3540) Lasers, Q-switched.

References and links

1. R. Bhandari and T. Taira, "> 6 MW peak power at 532 nm from passively Q-switched Nd:YAG/Cr⁴⁺:YAG microchip laser," *Opt. Express* **19**(20), 19135–19141 (2011).
2. Z. Zhuo, S. G. Li, T. Li, C. X. Shan, J. M. Jiang, B. Zhao, J. Li, and J. Z. Chen, "Diode-end-pumped passively Q-switched Nd:Y_{0.8}Lu_{0.2}VO₄ laser with Cr⁴⁺:YAG crystal," *Opt. Commun.* **283**(9), 1886–1888 (2010).
3. B. Y. Zhang, J. L. Xu, G. J. Wang, J. L. He, W. J. Wang, Q. L. Zhang, D. L. Sun, J. Q. Luo, and S. T. Yin, "Continuous-wave and passively Q-switched laser performance of a disordered Nd:GYSGG crystal," *Opt. Commun.* **284**(24), 5734–5737 (2011).
4. W. Z. Zhuang, W. C. Huang, Y. P. Huang, K. W. Su, and Y. F. Chen, "Passively Q-switched photonic crystal fiber laser and intracavity optical parametric oscillator," *Opt. Express* **18**(9), 8969–8975 (2010).
5. J. Liu, U. Griebner, V. Petrov, H. Zhang, J. Zhang, and J. Wang, "Efficient continuous-wave and Q-switched operation of a diode-pumped Yb:KLu(WO₄)₂ laser with self-Raman conversion," *Opt. Lett.* **30**(18), 2427–2429 (2005).
6. J. Dong, K. Ueda, and A. A. Kaminskii, "Efficient passively Q-switched Yb:LuAG microchip laser," *Opt. Lett.* **32**(22), 3266–3268 (2007).
7. D. S. Sumida and T. Y. Fan, "Effect of radiation trapping on fluorescence lifetime and emission cross section measurements in solid-state laser media," *Opt. Lett.* **19**(17), 1343–1345 (1994).
8. H. W. Bruesselbach, D. S. Sumida, R. A. Reeder, and R. W. Byren, "Low-heat high-power scaling using InGaAs-diode-pumped Yb:YAG lasers," *IEEE J. Sel. Top. Quantum Electron.* **3**(1), 105–116 (1997).
9. J. Dong, K. Ueda, A. Shirakawa, H. Yagi, T. Yanagitani, and A. A. Kaminskii, "Composite Yb:YAG/Cr⁴⁺:YAG ceramics picosecond microchip lasers," *Opt. Express* **15**(22), 14516–14523 (2007).
10. J. Dong, A. Shirakawa, K. Ueda, H. Yagi, T. Yanagitani, and A. A. Kaminskii, "Near-diffraction-limited passively Q-switched Yb:Y₃Al₅O₁₂ ceramic lasers with peak power >150kW," *Appl. Phys. Lett.* **90**(13), 131105 (2007).
11. J. Dong, A. Shirakawa, and K. Ueda, "Sub-nanosecond passively Q-switched Yb:YAG/Cr⁴⁺:YAG sandwiched microchip laser," *Appl. Phys. B* **85**(4), 513–518 (2006).
12. J. M. Hopkins, S. A. Smith, C. W. Jeon, H. D. Sun, D. Burns, S. Calvez, M. D. Dawson, T. Jouhti, and M. Pessa, "0.6 W CW GaInNAs vertical external-cavity surface emitting laser operating at 1.32 μ m," *Electron. Lett.* **40**(1), 30–31 (2004).
13. Y. Tzuk, A. Tal, S. Goldring, Y. Glick, E. Lebiush, G. Kaufman, and R. Lavi, "Diamond cooling of high-power diode-pumped solid-state lasers," *IEEE J. Quantum Electron.* **40**(3), 262–269 (2004).
14. P. Millar, A. J. Kemp, and D. Burns, "Power scaling of Nd:YVO₄ and Nd:GdVO₄ disk lasers using synthetic diamond as a heat spreader," *Opt. Lett.* **34**(6), 782–784 (2009).
15. P. Millar, R. B. Birch, A. J. Kemp, and D. Burns, "Synthetic diamond for intracavity thermal management in compact solid-state lasers," *IEEE J. Quantum Electron.* **44**(8), 709–717 (2008).

16. W. Koehler, *Solid State Laser Engineering* (Springer, 2006).
17. Y. Kalisky, C. Labbe, K. Waichman, L. Kravchik, U. Rachum, P. Deng, J. Xu, J. Dong, and W. Chen, "Passively Q-switched diode-pumped Yb:YAG laser using Cr⁴⁺-doped garnets," *Opt. Mater.* **19**(4), 403–413 (2002).
18. Q. Hao, W. Li, H. Pan, X. Zhang, B. Jiang, Y. Pan, and H. Zeng, "Laser-diode pumped 40-W Yb:YAG ceramic laser," *Opt. Express* **17**(20), 17734–17738 (2009).
19. J. Dong, J. Ma, Y. Cheng, Y. Y. Ren, K. Ueda, and A. A. Kaminskii, "Comparative study on enhancement of self-Q-switched Cr,Yb:YAG lasers by bonding Yb:YAG ceramic and crystal," *Laser Phys. Lett.* **8**(12), 845–852 (2011).
20. J. Dong, J. Li, S. Huang, A. Shirakawa, and K. Ueda, "Multi-longitudinal-mode oscillation of self-Q-switched Cr,Yb:YAG laser with a plano-concave resonator," *Opt. Commun.* **256**(1-3), 158–165 (2005).
21. J. Dong, A. Shirakawa, K. I. Ueda, and A. A. Kaminskii, "Effect of ytterbium concentration on cw Yb:YAG microchip laser performance at ambient temperature - Part I: Experiments," *Appl. Phys. B* **89**(2-3), 359–365 (2007).
22. J. Dong, A. Shirakawa, K. I. Ueda, and A. A. Kaminskii, "Effect of ytterbium concentration on cw Yb:YAG microchip laser performance at ambient temperature - Part II: Theoretical modeling," *Appl. Phys. B* **89**(2-3), 367–376 (2007).
23. D. C. Brown, "Ultrahigh-average-power diode-pumped Nd:YAG and Yb:YAG lasers," *IEEE J. Quantum Electron.* **33**(5), 861–873 (1997).
24. Q. Liu, X. Fu, M. Gong, and L. Huang, "Effects of the temperature dependence of the absorption coefficients in edge-pumped Yb:YAG slab lasers," *J. Opt. Soc. Am. B* **24**(9), 2081–2089 (2007).
25. J. Dong, M. Bass, Y. Mao, P. Deng, and F. Gan, "Dependence of the Yb³⁺ emission cross section and lifetime on temperature and concentration in yttrium aluminum garnet," *J. Opt. Soc. Am. B* **20**(9), 1975–1979 (2003).
26. T. Kasamatsu, H. Sekita, and Y. Kuwano, "Temperature dependence and optimization of 970-nm diode-pumped Yb:YAG and Yb:LuAG lasers," *Appl. Opt.* **38**(24), 5149–5153 (1999).
27. J. Dong and K. Ueda, "Temperature-tuning Yb:YAG microchip lasers," *Laser Phys. Lett.* **2**(9), 429–436 (2005).
28. M. Ostermeyer and A. Straesser, "Theoretical investigation of feasibility of Yb:YAG as laser material for nanosecond pulse emission with large energies in the Joule range," *Opt. Commun.* **274**(2), 422–428 (2007).
29. C. Li, Q. Liu, M. Gong, G. Chen, and P. Yan, "Q-switched operation of end-pumped Yb:YAG lasers with non-uniform temperature distribution," *Opt. Commun.* **231**(1-6), 331–341 (2004).
30. Y. F. Chen, K. W. Su, W. L. Chen, K. F. Huang, and Y. F. Chen, "High-peak-power optically pumped AlGaInAs eye-safe laser at 500-kHz repetition rate with an intracavity diamond heat spreader," *Appl. Phys. B* (to be published), doi:10.1007/s00340-012-4954-4.
31. Y. F. Chen, "High-power diode-pumped Q-switched intracavity frequency-doubled Nd:YVO₄ laser with a sandwich-type resonator," *Opt. Lett.* **24**(15), 1032–1034 (1999).
32. W. A. Clarkson and D. C. Hanna, "Efficient Nd:YAG laser end pumped by a 20-W diode-laser bar," *Opt. Lett.* **21**(12), 869–871 (1996).
33. J. J. Zayhowski, C. Dill III, C. Cook, and J. L. Daneu, "Mid-and high-power passively Q-switched microchip lasers," in *Proceeding of Advanced Solid-State Lasers*, M. M. Fejer, H. Injeyan, and U. Keller, eds., Vol. 26 of OSA Trends in Optics and Photonic Series (Optical Society of America, Washington, D. C., 1999), pp. 178–186.
34. J. J. Zayhowski, "Microchip lasers," *Opt. Mater.* **11**(2-3), 255–267 (1999).
35. J. J. Zayhowski, "Passively Q-switched Nd:YAG microchip lasers and applications," *J. Alloy. Comp.* **303–304**, 393–400 (2000).

1. Introduction

High-energy, compact diode-pumped passively Q-switched (PQS) solid state lasers with sub-nanosecond pulses have a variety of applications such as nonlinear frequency conversion, industrial processing, and remote sensing. Since Cr⁴⁺:YAG crystals possess high damage thresholds and high optical and thermal stabilities, they have been extensively applied as saturable absorbers in PQS laser systems such as Nd³⁺-doped lasers [1–3] and Yb³⁺-doped lasers [4–6]. Comparing with Nd:YAG crystals, Yb:YAG crystals have longer fluorescence lifetimes [7], smaller emission cross sections [8], low quantum defects, and broad absorption bandwidths [8]. Therefore, the Yb:YAG microchips have been employed to construct high-pulse-energy light sources with stability, compactness, and reliability [9–11].

The scaling of power and energy in Yb:YAG lasers are strongly impeded by the thermal effect because the quasi-three-level property of the Yb:YAG crystal causes the population on the lower level to significantly increase with rising temperatures. Therefore, efficient thermal management is highly desirable for enhancing the output performance of Yb:YAG PQS lasers. Recently, it has been demonstrated that the synthetic diamond is a promising heat spreader for thermal management in semiconductor disk lasers [12] and Nd-doped vanadate lasers [13–15] due to its excellent optical and mechanical properties together with high thermal conductivity. In addition, cooling along the direction of pumping is practically useful for reducing the thermal lensing and stress in microchip lasers [16, 17]. Even so, the

feasibility of cooling Yb:YAG microchip PQS lasers with diamond heat spreaders has never been explored thus far.

In this work, we explore the performance improvement of diode-end-pumped PQS Yb:YAG lasers with diamond windows as surface heat spreaders. Comparing with the results obtained without the diamond heat spreader, the pulse energy obtained with the diamond cooling is found to be enhanced by 1.5 times, where a Cr⁴⁺:YAG absorber with the initial transmission of 84% is used. Furthermore, the standard deviation of the pulse amplitude peak-to-peak fluctuation is approximately 3 times lower than that obtained without the diamond heat spreader. Under a pump power of 3.9 W, the passively Q-switched Yb:YAG laser can generate a pulse train of 3.3 kHz repetition rate with a pulse energy of 287 μJ and with a pulse width of 650 ps. More importantly, the optical-to-optical efficiencies are improved up to 58% and 25% for the continuous-wave (CW) and PQS operations, respectively.

2. Experimental setup

Figure 1 presents the schematic experimental setup. The gain medium was a 1-mm-long, 4 mm in diameter, and 11 at.% doped Yb:YAG crystal. One of the end facet of the crystal was coated with highly reflectivity (HR, R>98%) at 1030 nm and high-transmission (HT, T>95%) at 970 nm served as the front mirror, the other facet was with high-transmission (HT, T>95%) at 1030 nm and highly reflectivity (HR, R>95%) at 970 nm to increase the absorption efficiency of the pump power. The Cr⁴⁺:YAG crystal with initial transmission (T₀) of 84% and 1.4 mm in length was used as the saturable absorber. Both end facets of the Cr⁴⁺:YAG crystal were anti-reflection coated (AR, R<0.2%) at 1030 nm. The output coupler was a flat mirror with partially reflection at 1030 nm (R = 30%). The total cavity length was about 8.4 mm. The uncoated, single crystal synthetic diamond of 4.5 mm square and 0.5 mm thickness was used as the heat spreader and bounded to the front mirror side of the gain medium. The diamond plate was polished to laser quality with flatness of λ/8 at 632.8 nm and roughness of Ra smaller than 30 nm. The other side of the diamond was in contact with a copper heat sink cooled by a thermal-electric cooler at the temperature of 16°C. The side of the Yb:YAG crystal with the coating of HT at 1030 nm and HR at 970 nm was attached tightly to a copper plate with a hole of 2-mm diameter, where an indium foil was used to be the contact interface. The contact uniformity of the bounded interface between the diamond and the Yb:YAG crystal was further confirmed by means of inspecting the interference fringe resulting from the minute gap between the diamond heat spreader and the gain medium. The birefringence of the single crystal diamond was smaller than 5×10⁻⁴. The transmittance of the diamond heat spreader was about 70% at 970 nm owing to the high refractive index contrasts of the air/diamond and diamond/Yb:YAG interfaces (The refractive index of the single crystal diamond is 2.432). The Cr⁴⁺:YAG crystal was wrapped within indium foil and mounted in a copper heat sink cooled by water at the temperature of 16°C. The pump source was an 8-W 970-nm fiber-coupled laser diode with a core diameter of 200 μm and a numerical aperture of 0.20. Focusing lens with 25 mm focal length and 87% coupling efficiency is used to reimage the pump beam into the laser crystal. The pump diameter is approximately 120 μm. Considering the coupling efficiency of the focusing lens, the transmittance of the diamond, and the effective absorption of the gain medium, the maximum available absorbed pump power is found to be 3.9 W. Note that without using the diamond heat spreader the maximum available absorbed pump power can be up to 5.6 W. The laser spectrum was measured by an optical spectrum analyzer with 0.1 nm resolution (Advantest Q8381A). The pulse temporal behavior was recorded by Agilent digital oscilloscope (infiniium DSO81204B; 40G samples/sec; 12 GHz bandwidth) with a fast InGaAs photodiode of 12.5 GHz bandwidth.

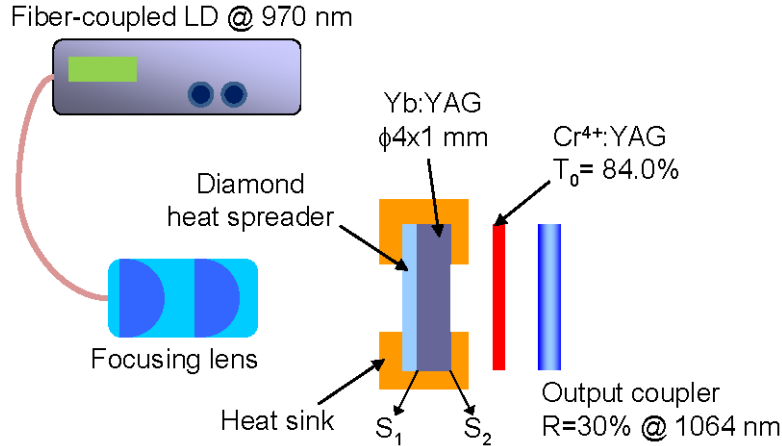


Fig. 1. The schematic diagram of the PQS Yb:YAG/Cr⁴⁺:YAG laser experimental setup. (S₁: HT at 970 nm, HR at 1030 nm; S₂: HT at 1030 nm, HR at 970 nm; HT: high transmission; HR: high reflection).

3. Experimental results and discussion

We firstly investigate the performance of the Yb:YAG laser with the diamond heat spreader under CW operation without the Cr⁴⁺:YAG crystal in place. Here, we use the output coupler with reflectivity of 80% at 1030 nm to maximize the output power around the wavelength of 1031 nm under CW operation. Figure 2 shows the average power with and without the diamond heat spreader with respect to the absorbed pump power. Without the diamond heat spreader, the output power was 1.3 W under an absorbed pump power of 3.9 W which corresponds to the optical-to-optical efficiency of 33% and the slope efficiency of 50%. The output power started to saturate and the slope efficiency decreased to 17% for an absorbed pump power of 5.6 W. The thermal effects induced power degradation has been widely observed in Yb-doped lasers [18–21] and has been theoretically confirmed [22]. Increasing the pump power, the detrimental effects in the Yb:YAG crystal become more severe including the decrease of the thermal conductivity [22] and the increase of the thermal expansion coefficient [23]. Furthermore, the absorption cross section and the emission cross section of the transitions between the manifolds ²F_{5/2} and ²F_{7/2} in the Yb:YAG crystal are significantly decreased with the increased temperature [24, 25] which lead to the reduction of the laser efficiency [16]. In contrast, the maximum output power was enhanced to 2.25 W under the pump power of 3.9 W when a diamond heat spreader was employed for surface cooling. The optical-to-optical efficiency and the slope efficiency were up to 58% and 86%, respectively.

Under the PQS operation, we change the reflectivity of the output coupler to be 30% at 1030 nm to prevent coating damages of the crystals due to the high intracavity intensity which have been observed in PQS Yb:YAG/Cr⁴⁺:YAG lasers [11]. Figure 3(a) depicts the averaged output power versus absorbed pump power under the PQS operation. Without the diamond heat spreader, the maximum output power was found to be limited at 0.47 W under the absorbed pump power of 5.6 W. Like the CW operation, the averaged output power without diamond cooling began to saturate when the absorbed pump power was greater than 4.5 W. On the contrary, the average output power with diamond cooling was 0.96 W at an absorbed pump power of 3.9 W, corresponding to the optical efficiency of 25% and the slope efficiency of 60%. Lower temperature in the Yb:YAG crystal can achieve lower threshold pump power [26] and higher optical efficiency [27] in Yb:YAG lasers. The lower threshold pump power (2.3 W for with diamond heat spreader and 2.8 W for without diamond heat spreader) and higher optical efficiency (25% for with diamond heat spreader and 8.3% for without diamond heat spreader) attained in our results show the effective thermal management of the diamond heat spreader. In comparison with the earlier results such as the self-Q-switched laser that

uses composite Yb:YAG/Cr⁴⁺:YAG ceramics [9] and the mechanical contacted Yb:YAG/Cr⁴⁺:YAG microchip lasers that adopt ceramics [10] or crystals [11], the diamond cooling scheme is confirmed to enhance the performance significantly. The lasing spectra for CW and PQS operations with the diamond heat spreader were quite similar with the peaks near 1031.7 nm and bandwidths to be approximately 0.2 nm, as shown in the inset of Fig. 3(a).

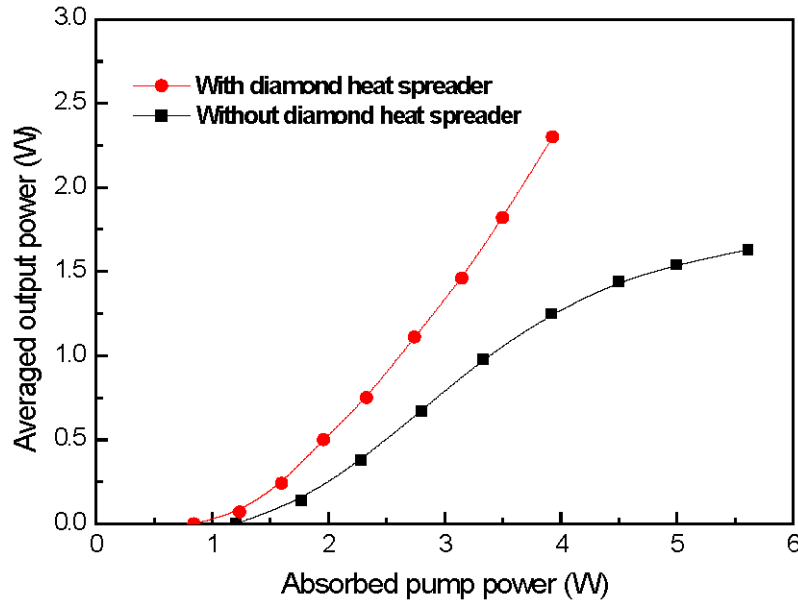


Fig. 2. Dependence of the averaged output power on the absorbed pump power under the CW operation.

Figure 3(b) shows the pulse energies obtained with and without the diamond heat spreader with respect to the absorbed pump power. It can be seen that the maximum pulse energies obtained without and with diamond cooling are approximately 190 μ J and 287 μ J, respectively. The Yb:YAG crystal, as a quasi-three-level laser gain medium, certainly suffers from the increase of the fractional thermal population on the lower laser level and the decrease of the fractional population on the upper laser level which decrease the maximum stored energy in the Yb:YAG crystal [28] for increasing the pump power. Furthermore, the strong thermal lensing in the end-pumped Yb:YAG microchip laser which results from the thermal gradients within the gain medium [17] usually leads to a smaller cavity mode size that will reduce the output pulse energy [29]. Millar et al. [15] and our previous results [30] in semiconductor disk lasers which use diamond heat spreader for thermal management of the gain medium have evidence its effectualness. Smaller red-shift in wavelength when the diamond heat spreader was in place [15, 30] confirms that the gain medium heating to be considerably improved by using the diamond heat spreader. By using the same diamond heat spreader and the same bounding method of the diamond/gain medium composite as in this experiment, our previous result [30] shows that the gain medium temperature rise per unit pump power ($\Delta T/\Delta P$) are 20.5 K/W and 3.3 K/W for without and with the diamond heat spreader. The temperature rise in the diamond-gain medium composite is 6.2 times lower than in the gain medium without a diamond heat spreader, emphasizing the efficiency of the diamond heat spreader for thermal management. Besides, Millar et al. [15] theoretically simulates that using the diamond heat spreader can effectively reduce the maximum temperature rise together with temperature gradients and decrease the thermal stress and distortion in Yb:YAG lasers. Our experimental results confirm that diamond cooling is truly an efficient thermal management for the Yb:YAG microchip laser to enhance the output

performance. To the best of our knowledge, this is the highest pulse energy obtained with Yb:YAG/Cr⁴⁺:YAG microchip laser. The overall pulse energy scaling was 1.9 times as high as the one in Ref [9], 5.7 times as that in Ref [10], and 22 times as that in Ref [11]. The diamond heat spreader not only reduces the maximum temperature rise in the gain medium to enhance the laser efficiency but also decreases the thermal-induced bending and bowing of the gain medium to improve the beam distortion [15, 16]. Furthermore, bounding the diamond heat spreader to the pumped side of the gain medium makes the temperature distribution more uniform [16] that reduces the thermal lens in the Yb:YAG crystal and prevents the cavity mode size from shrinking as the result of the thermal lens effect [31, 32].

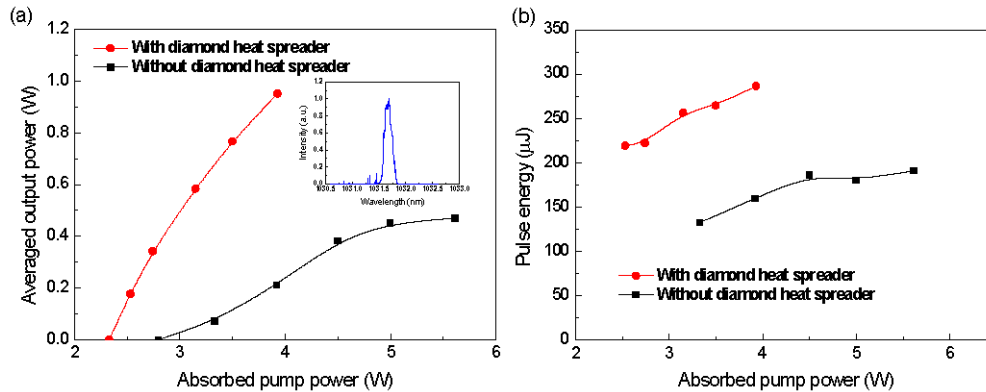


Fig. 3. (a) Dependence of the averaged output power on the absorbed pump power under the PQS operation, the inset: typical lasing spectrum. (b) Dependence of the pulse energy on the absorbed pump power.

Figures 4(a) and 4(b) show the oscilloscope traces obtained with and without diamond cooling, respectively, for the single pulse of the PQS Yb:YAG/Cr⁴⁺:YAG laser at the maximum absorbed pump powers. The pulse widths can be seen to be 650 ps and 764 ps for the operations with and without diamond cooling, respectively. With the pulse energy shown in Fig. 3(b), the peak powers obtained with and without diamond cooling can be calculated to be 442 kW and 262 kW, respectively. In other words, diamond cooling enhances the peak power by a factor of 1.7 times.

Zayhowski et al. demonstrated PQS microchip lasers constructed of diffusion-bounded Nd:YAG/Cr⁴⁺:YAG crystals [33–35]. By optically bounding a 4-mm-long Nd:YAG crystal doped with 1.1 at.% Nd³⁺ ions and a 2.25-mm-thick Cr⁴⁺:YAG, laser pulses with pulse energy of 250 μJ and pulse width of 380 ps at the pulse repetition rate of 1 kHz were obtained under 15 W of pump power, the corresponding peak power of 565 kW was attained. Compared to our result of Yb:YAG/Cr⁴⁺:YAG laser, although the pulse width achieved by Nd:YAG/Cr⁴⁺:YAG laser was shorter than ours owing to the shorter laser resonator, the optical-to-optical efficiency was less than 2% which was much inferior to ours of 25%. Besides, the Nd:YAG/Cr⁴⁺:YAG laser can only be pulse pumped which limited the pulse repetition rate to be merely up to 1 kHz as the result of the thermal effects. At higher repetition rates, the pulse energy of the Nd:YAG/Cr⁴⁺:YAG laser decreased due to the cavity mode shrinking induced by the thermal lens effect. The output pulses start to bifurcate with varied pulse amplitudes in different longitudinal and polarization modes when the laser was CW pumped [33]. Our results provide the solution for improved thermal management by using a diamond heat spreader in the Yb:YAG/Cr⁴⁺:YAG laser, nevertheless, this method also can be expected to be useful in the Nd:YAG/Cr⁴⁺:YAG system.

Figures 5(a) and 5(b) depict the typical oscilloscope traces measured with and without the diamond heat spreader, respectively, for the Q-switched pulse trains at the maximum absorbed pump powers. The standard deviations of the pulse amplitude peak-to-peak fluctuations are analyzed to be approximately 3% and 9% for the operations with and without

the diamond heat spreader, respectively. The pulse amplitude fluctuation with the heat spreader is also superior to the earlier results such as 6% in Ref [9], and 8% in Ref [10], demonstrating an effective improvement in the PQS stability.

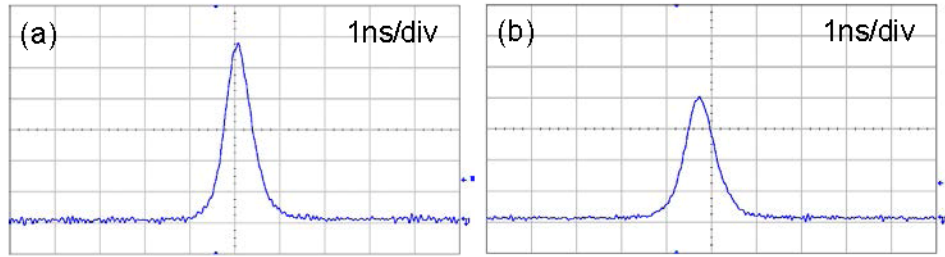


Fig. 4. Oscilloscope traces of a single pulse of the output pulse of (a) with the diamond heat spreader, (b) without the diamond heat spreader.

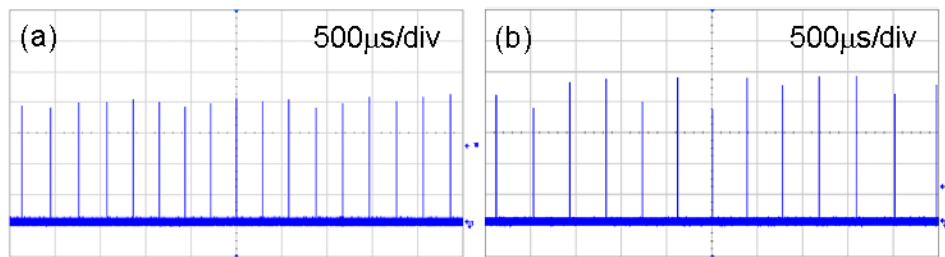


Fig. 5. Oscilloscope traces of a train of output pulses of (a) with the diamond heat spreader, (b) without the diamond heat spreader.

4. Conclusions

We have experimentally confirmed that employing diamond windows as surface heat spreaders can remarkably improve the performance of diode-end-pumped PQS Yb:YAG lasers. The pulse energy obtained with the diamond cooling was found to be 1.5 times higher than that obtained without the diamond heat spreader, where a Cr⁴⁺:YAG absorber with the initial transmission of 84% was employed in experiment. Under a pump power of 3.9 W, a pulse train of 3.3 kHz repetition rate could be efficiently generated from the passively Q-switched Yb:YAG laser with a pulse energy of 287 μJ and with a pulse width of 650 ps. In addition, the optical-to-optical efficiencies were found to be improved up to 58% and 25% for the CW and PQS operations, respectively. The standard deviations of the pulse amplitude peak-to-peak fluctuations were measured to be approximately 3% and 9% for the operations with and without the diamond heat spreader, respectively. This result indicates that the amplitude fluctuation obtained with diamond cooling was approximately 3 times lower than that obtained without diamond cooling.

Acknowledgments

The author thanks the National Science Council for their financial support of this research under Contract No. NSC100-2628-M-009-001-MY3.